Chemical Physics Letters 465 (2008) 147–152

Contents lists available at ScienceDirect

Chemical Physics Letters

journal homepage: www.elsevier.com/locate/cplett

Direct measurement of diffusion in liquid phase by electron spin resonance

Aharon Blank [a,*], Yael Talmon [a], Michael Shklyar [a], Lazar Shtirberg [a], Wolfgang Harneit [b]

[a] Schulich Faculty of Chemistry, Technion – Israel Institute of Technology, Technion City, Haifa 32000, Israel
[b] Institut für Experimentalphysik, Freie Universität Berlin, Arnimallee 14, 214195 Berlin, Germany

ARTICLE INFO

Article history:
Received 15 July 2008
In final form 22 September 2008
Available online 26 September 2008

ABSTRACT

Pulsed-gradient spin-echo (PGSE) NMR is a powerful technique that can directly measure the self-diffusion coefficient of molecules in a variety of environments. PGSE NMR can typically measure motions of at least $\sim 10^{15}$ molecules in the milliseconds-to-seconds time scale. Here we demonstrate for the first time that through the use of a unique miniature resonator and powerful and rapid gradient sources, electron spin resonance (ESR) can also be employed to measure diffusion in liquid state. The PGSE ESR method, which operates at the microseconds time scale with much higher molecular sensitivity, can complement and enhance the current capabilities of NMR.

© 2008 Elsevier B.V. All rights reserved.

1. Introduction

The measurement of translational motion is one of the most fundamental types of observation in science. Over the last four decades, PGSE has been employed in conjunction with liquid-state nuclear magnetic resonance (NMR) for the measurements of motion in applications ranging from basic materials science to medical diagnosis. It is considered to be one of the most accurate and versatile methods for diffusion measurement [1,2]. One of the main unique features of PGSE NMR is its capability to measure restricted and anisotropic diffusion in various media which can lead, for example, to the characterization of complex porous structures [3–6]. The limited sensitivity and the relatively long time scales of the processes in liquid-state NMR directly affect PGSE NMR capabilities; typically, it measures collective motions occurring in the milliseconds-to-seconds time scale over distances larger than $\sim$0.1 μm and only for $\sim 10^{15}$ molecules or more [7]. Other methods used for the measurement of translational motion are neutron scattering [8], optical fluorescence photobleaching [9], fluorescence correlation spectroscopy [10], and single molecule tracking [11]. These methods are complementary to PGSE NMR in terms of the temporal and the spatial resolution. For example, neutron scattering can monitor motions occurring in the time scales of 10^{-13}–10^{-7} s and extending to a range of up to $\sim$100 Å [8,12]. Optical fluorescence tracking of a single molecule has time resolution in the milliseconds range and can observe movements over distances that must be larger than a few tens of nanometers [11]. Fluorescence photo bleaching has similar capabilities and mainly observes the collective motion of many molecules, while fluorescence correlation spectroscopy can monitor diffusion occurring during intervals as short as several microseconds and distances of $\sim$0.2 μm, but only for very low (<1 nm) molecular concentrations [10] and it is very sensitive to a variety of experimental conditions [13]. In general, the resolution of optical methods (up to $\sim$0.1 μm), limits the *accurate* measurement of the diffusion to motions that are at least five times larger than the resolution ($\sim$0.5 μm) (for example, see [14]). In the context of techniques for motion measurement we can also mention *indirect* methods for molecular dynamics estimation, such as the analysis of NMR and ESR spectrum for the extraction of relaxation and order parameters data [15,16], and the extraction of diffusion from ESR [17] and fluorescence data [18,19] for processes which involve molecular collision. Fig. 1 provides a graphical summary of the capabilities of the methods described above for the *direct* measurement of diffusion. It should be noted that although in some respects optical methods overlap with the capabilities of PGSE NMR, they are still limited in handling many applications involving non-transparent samples, samples with anisotropic and/or restricted diffusion, and samples with complex (multi-component) diffusion.

In view of the above, it is evident that despite the considerable progress in all of these methods there are still many gaps in the existing capabilities to directly measure motion, especially for common inter- and intra-molecular and biological processes occurring in the time scale of 10^{-7}–10^{-4} s. This time scale is not accessible by NMR but could be naturally addressed through the analogue method of PGSE ESR. ESR operates in the microseconds time scale and thus can be complementary to the existing methods, especially to the NMR-based approaches. Furthermore, the greater sensitivity (up to $\sim 10^7$ molecules) and specificity (using stable free radicals or spin labels – similar to fluorescent labels in optics) of the ESR technique at ambient conditions can be of importance in many biological and materials science applications. In this work we demonstrate for the first time that PGSE ESR can be

* Corresponding author. Fax: +972 4 829 5948.
E-mail address: ab359@tx.technion.ac.il (A. Blank).

0009-2614/$ - see front matter © 2008 Elsevier B.V. All rights reserved.
doi:10.1016/j.cplett.2008.09.052

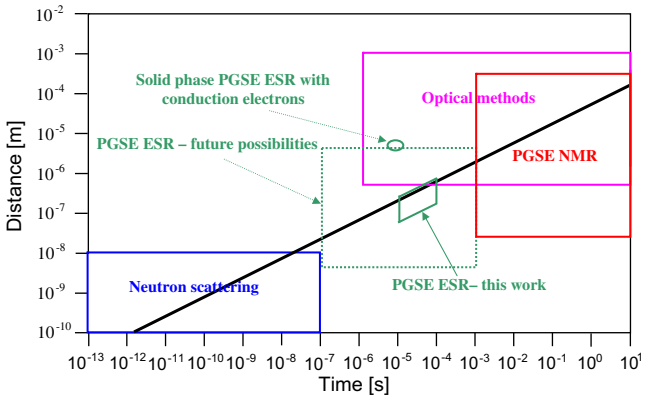

Fig. 1. Graphical summary of the motion measurement capabilities for the various methods described in the text (rough outline). The horizontal axis represents the characteristic time in which the motion can be tracked while the vertical axis represents the length scale of the motion during that time. The black line represents the diffusion length ($\sqrt{4Dt}$) for $D = 1 \times 10^{-9}$ m^2/s, which is characteristics to aqueous environment.

employed to measure translation motion in a *liquid phase*, and thus provide in principle 'PGSE NMR-type' information in time-distance scales that are beyond the reach of current methods.

ESR is a common and commercially available technique. Nevertheless, due to extreme technical challenges, PGSE has never been applied in conjunction with ESR to the measurement of motion in a liquid phase. The main difficulty lies in the requirement to apply very strong magnetic field gradients over very short periods of time. This requirement can be explained quantitatively by investigating the equation that describes the measured echo signal in a typical PGSE experiment [2]:

$$E_{(t=2\tau_2+\tau_1)} = A\exp(-2\tau_2/T_2 - \tau_1/T_1 - D\gamma^2 g^2 \delta^2(\Delta - \delta/3)) \quad (1)$$

where A describes the maximum amplitude of the echo, T_1 and T_2 are the spin–lattice and spin–spin relaxation times of the measured radical, respectively, D is the diffusion constant, γ is the electron gyromagnetic ratio and the pulse-related parameters τ_1, τ_2, Δ, δ, g are defined in Fig. 2. In order to properly quantify the value of D, the attenuation of the echo signal due to the last term in the argument of the exponential must be dominant with respect to the first two terms. This condition is best met with species having relatively long relaxation times (T_1 and T_2). However, even if one considers unique soluble radicals with extremely long relaxation times, such as the perdeuterated trityl ($T_1 \sim 17$ μs, $T_2 \sim 11$ μs) [20], to significantly affect the echo amplitude and enable the measurement of D in a liquid phase, with typical values of $2\tau_2/T_2 = 0.5$ and $\tau_1/T_1 = 0.5$, the required pulsed gradients must reach a level of ~50 T/m. Applying such high gradients over a short duration of several microseconds is highly challenging and for many years was well beyond the state-of-the-art. For example, in NMR, the most advanced pulse experiments were able to achieve gradients that are as high as 50 T/m, but over a much longer duration of ~1 ms [21]. Another difficulty lies in the need to produce the two gradient pulses (Fig. 2) with identical integrals up to a numerical factor that is the ratio between the smallest measured movement and the size of the sample. (For example, to monitor movements of 0.1 μm with a typical ESR/NMR sample size of 10000 μm, the two pulses must be matched up to 0.1/10000 = 10 ppm difference [1].) These combined experiential difficulties prevented, up to now, the observation of the PGSE phenomenon in liquid-phase ESR.

Solid-phase ESR does offer several examples of the measurement of anisotropic motion with ESR, either by constant read gradient [22] or by PGSE [23]. However, these measurements were carried out on the conduction electrons of a unique organic conductors, which are characterised by very long spin relaxation times and, most importantly, a diffusion constant that is more than three orders of magnitude larger ($D \sim 10^{-6}$ m^2/s) than that of common solutions. Another example of the direct measurement of diffusion using ESR, without PGSE, is based on introducing a concentration singularity in a liquid sample and monitoring the signal changes over time scales of several seconds [24].

The experimental work described in this letter has overcome the challenges of producing strong and short gradients, while relaxing the requirement for identical gradient pulses somewhat by using relatively small samples. Here we present PGSE ESR measurements which for the first time directly measure the motion (diffusion coefficient) of molecules in a *liquid solution*. We obtained the diffusion coefficient of two different spin systems in various solvents (a total of three types of samples). The first two included a saturated solution of the N@C_{60} molecular electron spin system [25] in 1-cholornaphtalene and CS_2. The third sample was made of 1 mM deuterated trityl radical in water [20]. These spin systems were chosen for their long relaxation times and their potential use for many applications (see below). This new capability paves the way to monitoring in the near future motions occurring in the time scale of 10^{-7}–10^{-4} s, over distances that can be as short as several nanometers.

2. Experimental details

2.1. Materials and samples preparation

N@C_{60} was synthesized by continuous nitrogen ion implantation into freshly sublimed fullerene layers with a yield (N@C_{60}:C_{60} ratio) of ~0.01% as described elsewhere [25] The N@C_{60} contained in the harvested product was enriched and

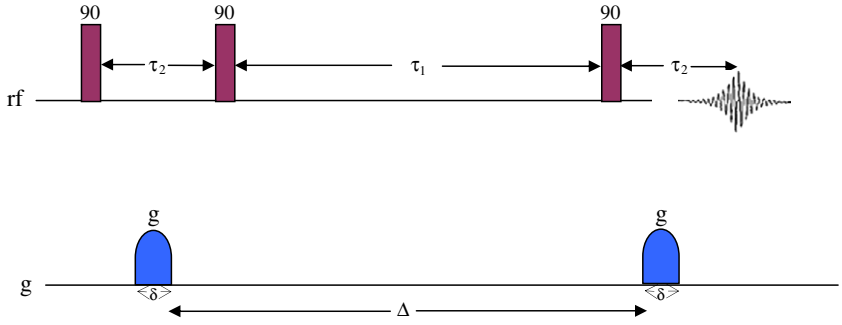

Fig. 2. Pulse sequence for stimulated echo pulsed gradient employed in the present work. The half sin shaped pulsed field gradients have varying amplitude (g) and a typical duration of δ. Phase cycling scheme with 16-steps was used to cancel all unwanted FID and echo signals [36].

purified by multi-step high-pressure liquid chromatography (HPLC) [26]. Sample purity was checked by UV–vis absorption and analytical HPLC. The fullerene content of the sample is estimated to be better than 99.5%, consisting mostly of diamagnetic species C_{60} (83.7%), its epoxide $C_{60}O$ (14.4%), and trace amounts (<0.3%) of C_{70}. The $N@C_{60}/C_{60}$ ratio of 1.6(3)% was quantified using analytical HLPC and electron spin resonance as described earlier [27].

The enriched $N@C_{60}$ sample was dissolved in Carbon Disulfide (99.9%–from Spectrum chemicals), which resulted in room temperature saturated solution concentration of ~0.15 mM (for the $N@C_{60}$). The solution was then placed in a ~0.5-mm i.d. capillary glass tube and evaporated slowly to increase its concentration (up to the level of saturation). $N@C_{60}$ in 1-chloronaphthalene was prepared by taking a sample of $N@C_{60}$ in CS_2, evaporating the solvent completely and then adding a small amount of 1-chloronaphthalene (90% from ACROS organics) to the tube. Here the saturated solution concentration of $N@C_{60}$ was ~1.1 mM. Both $N@C_{60}$ samples tubes were sealed under normal atmosphere.

Solid $N@C_{60}$ sample with $N@C_{60}/C_{60}$ ratio of 0.1% was prepared by mixing the enriched $N@C_{60}$ in CS_2 with pure C_{60} solution in the appropriate ratio, and drying the solvent.

The sample of the trityl radical (courtesy of Dr. Wistrand, Nycomed Sweden) was made by preparing a 1 mM solution in distilled water, transferring it to a capillary glass tube and then sealing it in vacuum (after several freeze thaw cycles – to remove excessive O_2).

The number of spins in the samples was calculated on the basis of their concentration and the sample volume inside the resonator (~0.5 mm high) and was found to be $\sim 6 \times 10^{13}$, 9×10^{12}, and 9×10^{12} for the $N@C_{60}$ in 1-chloronaphthalene, CS_2 and the trityl in water, respectively.

2.2. Experimental setup

The PGSE ESR experiments and the measurements of the sample's T_1 and T_2 were all carried out with our 'home-built' pulsed ESR imaging system. The block diagram of the experimental system is presented in Fig. 3. The system is constructed from the following main components: (a) a PC that controls the image acquisition process through LabView software (National Instruments); (b) a timing card (PulseBlasterESR-Pro by SpinCore) with 21 TTL outputs, a time resolution of 2.5 ns and a minimum pulse length of 2.5 ns; (c) an 8-bit, two-channels PCI-format digitizer card for raw data acquisition and averaging, with a sampling rate of 500 MHz and averaging capability of up to 0.7 M waveforms/s (AP-235, Acqiris); (d) two PCI analog output cards, each having 8 outputs with 16-bit resolution (PCI-6733, National Instruments) that determine the gradient values; (e) a microwave reference source (HP8672A) with power output of 10 dBm in the 2–18 GHz range; (f) a 'home-built' pulsed microwave bridge containing (g) a 6–18 GHz low-power transceiver and (h) a solid-state power amplifier with 1 W output, 35 dB gain (home made); (i) a high-voltage pre-regulator power supply for the gradient coil drivers (j), which controls the pulsed gradient coils in the imaging probe; (k) a micro-imaging probe.

The micro-imaging probe and its gradient coils are shown in Fig. 4. They are an improved version of the probe described before [28] and constitute most of the key components that ultimately enabled the diffusion measurements presented here. At the centre of the probe we find a Rutile (TiO_2) microwave single ring dielectric resonator with an outer diameter of 2.4 mm, inner diameter of 0.9 mm and a height of 0.5 mm that is fed by a coaxial line. The resonator is placed with the sample at the center of the gradient coils structure. The gradients include a set of x-, y-, and z-gradient coils. The structure of the x-gradient coil is based on a simple Maxwell pair, the coils of the pair are connected in parallel and have a total inductance of 1.1 μH, a resistance of 0.5 Ohm, and produce a magnetic gradient of 1.42 T/mA. The y-gradient coil is based on Golay geometry, has a total inductance of 2.09 μH, a resistance of 0.55 Ohm, and produces a magnetic gradient of 1.25 T/mA. Both the x- and y-gradient coils are driven by the pulse current drivers. The z-gradient coil is also based on Golay geometry, but with serial connection between the upper and lower parts of the coil and has an efficiency of 1.31 T/mA. Its total inductance is 8.9 μH and its resistance is 1.8 Ohm (it was not used in this work). The strength of the gradients was calculated by a 'home made' Matlab software, based on Biot-Savart law. The calculations were verified experimentally (for the x- and y-gradient coils) by applying a constant (DC) 0.1 A of current directly into the gradient coils and measuring the broadening of the $N@C_{60}$ sample ESR signal in the frequency domain. By knowledge of the size of the sample one can directly calculate from the signal broadening the gradient strength for 1 A of drive current. The shield (shown in Fig. 4, made of ~1 μm thick golden foil) acts as a barrier which prevents the microwave from escaping out of the resonator but still enables the low

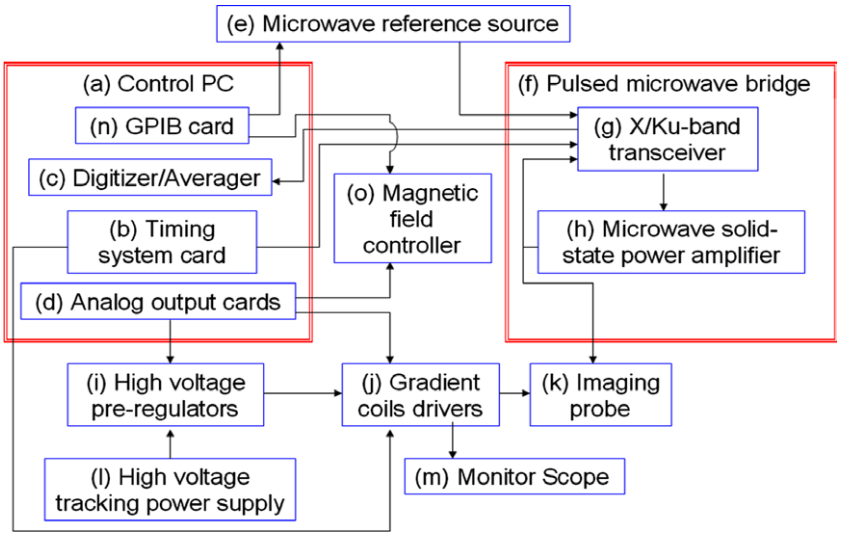

Fig. 3. Block diagram of the ESR system employed in the present work.

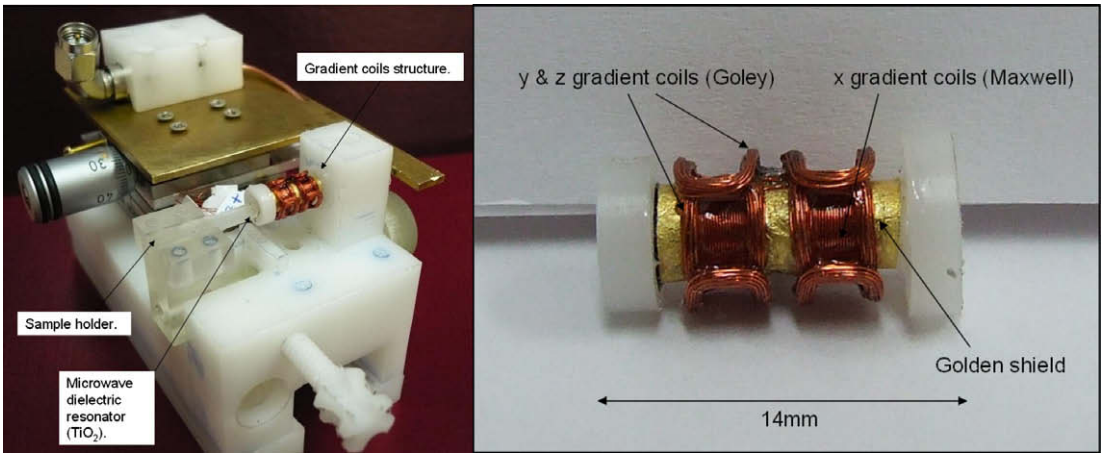

Fig. 4. ESR micro imaging probe employed in the present work. General view of the probe structure with the tiny resonator taken outside the gradient coil structure (left). Detailed view of the miniature gradient coils set (right).

frequency field generated by the gradient coils to penetrate inside. This enables maintaining a high quality factor for the microwave resonator, while still avoiding eddy currents due to the fast pulsed gradients. In the PGSE experiments, the *x*-axis coil was used for the main gradient pulses, while the *y*-axis coil was fed by a small DC current (~0.02 A). The constant y-gradient adds a small artificial inhomogenous broadening to the signal, without affecting T_1 and T_2 values. This enables better cancelation of the residual free induction decay (FID) signal from the last pulse (in addition to the use of phase cycling for the FID cancelation). Furthermore, the induced small inhomogenous broadening (~0.015 mT) results in a more stable signal in our system, which has field stability of ~0.002 mT that is marginal for the measurements of radicals with long T_2. The effect of this constant y-gradient ($g \sim 0.025$ T/m) on the echo signal attenuation due to diffusing is negligible (see Eq. (1)).

Additional key components that enable the diffusion measurement capability and deserve more attention are the pulsed gradient current drivers. These units are an improved version of the system described in [29] that operates by producing short intense current pulses into the gradient coils by means of a capacitor discharge. In our present system the peak current of the drivers can reach an output of 40 A (out of a 620 V source) with short pulses of 0.5–1 μs. This is a significant improvement over previous efforts where peak currents of only few amps were available for the same or longer pulse durations [28,29]. The capabilities of the gradient drivers along with the small size and the high efficiency of the gradient coils resulted in maximum available gradient of ~55 T/m for typical duration of ~0.8 μs. All measurements were carried out at a room temperature of ~ 24 °C.

2.3. T_1 and T_2 measurements

In order to complement the data regarding our samples we conducted a set of T_1 and T_2 measurements, which yielded the following results: for N@C_{60} in 1-chloronaphthalene T_1 and T_2 were found to be 33.3 and 6.4 μs, respectively. For N@C_{60} in CS_2 the measured values are 91 and 14.3 μs, and for trityl in water 16.7 and 5 μs. For the solid N@C_{60} sample with N@C_{60}/C_{60} ratio of 0.1% we measured T_1 and T_2 of 80 μs and 2.85 μs. The values of T_1 were calculated from the data obtained during stimulated echo measurements (see Fig. 2) with a constant τ_2 and varying values of τ_1 (via an exponential line fit). The values of T_2 were measured by a simple two pulse Hahn echo sequence with an 8-step phase cycle (CYCLOPS and FID cancelation).

3. Results and discussion

3.1. Preliminary observations and testing

The system underwent several stages of testing and optimization prior to the actual diffusion measurements. The main challenge, other than the construction of the micro-ESR probe and gradient drivers, was to reduce to a minimum the residual magnetic fields that follow such intense and short gradient pulses. The use of a miniature dielectric (non-metallic) resonator greatly attenuates these transient effects. Furthermore it also increases significantly the signal from such small sub-micro-litre samples [30] (leading to less stringent requirements for the identity of the pair of gradient pulses – as discussed above). However, these measures do not solve all the problems; there are still some residual fields that are caused by the current in the gradient coil itself as well as by transient 'eddy currents' in the auxiliary gradient coils of the probe (Fig. 4). The residual current after each pulse in the x gradient coil (Fig. 5) was minimized through the design of the electronic driver circuit and by minimizing the inductance of this coil and reducing the capacitance of the transmission line. Other transient magnetic fields at the position of the sample were found to be

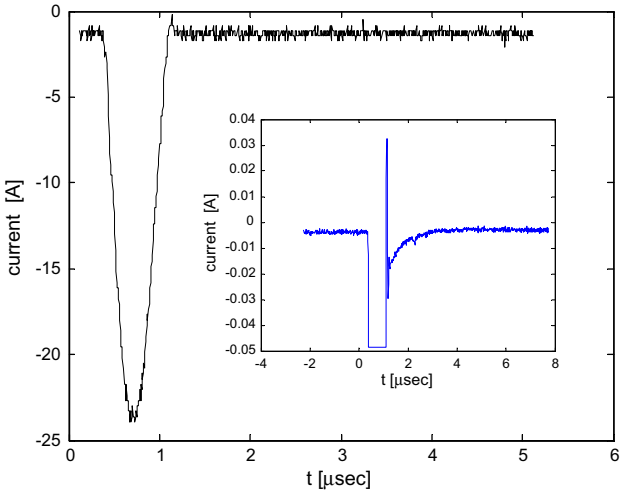

Fig. 5. Recording of a typical current drive during the pulsed field gradient. The duration of the pulse is ~0.8 μs. The insert shows the relatively fast decay and pulse behaviour in the trailing edge.

generated by residual currents in the auxiliary y-gradient coil. In order to measure the overall effect of all unwanted transient magnetic fields, the stimulated echo magnitude was monitored with and without gradient pulses. Ideally, when the diffusion effect is negligible, the same echo signal magnitude should be obtainable with and without the gradients (complete 'signal reconstruction'). In practice, however, this is not the case and the level of 'signal reconstruction' depends on various parameters such as the values of τ_1 and τ_2 in the pulse sequence, strength and duration of gradients, and sample dimensions. In the present setup we employed two types of samples to test this signal reconstruction efficiency: a sample of N@C_{60} in 1-chloronaphthalene, which is very viscous, and a solid N@C_{60} sample with N@C_{60}/C_{60} ratio of 0.1%. As an example for the results of these tests, with typical values of τ_2 = 2.5 μs and τ_1 = 40 μs, when using a 30 T/m gradient pulse that is 0.8 μs long, about 62% and 64% of the echo signal was reconstructed for the viscous liquid and solid samples, respectively. When the gradient peak value was increased to 50 T/m (while keeping all other parameters constant), only about 14% and 15% of the echo signal was reconstructed for the liquid and solid samples, respectively. (It should be noted that under these conditions, the contribution from diffusion in the viscous liquid sample to echo decay is very small and should reduce its magnitude to a level that is to the most ~90% of the full echo amplitude – see below.) These figures are not ideal but were more than enough to perform our measurements, when properly taken into consideration.

3.2. Experimental results

Two types of measurements were carried out in the present work. In the first, the stimulated echo was recorded for constant τ_2 and varying values of τ_1 (Fig. 2). In such a measurement the ratio of the stimulated echo signal with gradient pulses to that without gradients represents the combined effect of the residual transient magnetic fields and the diffusion-related signal decay. The effect of signal decay due to the residual transient magnetic fields was found to be the same for all values of τ_1 (for constant τ_2) and thus could be compensated by simple normalization. In contrast to that, the effect of diffusion on signal decay should increase as τ_1 is increased, making it possible to evaluate the diffusion coefficient in a straightforward manner, based on Eq. (1). The results of this type of measurement, carried out with τ_2 = 2.5 μs and a peak gradient of 30 T/m, are shown in Fig. 6a. The theoretical graphs for both N@C_{60} samples were plotted without any fitting, simply by using Eq. (1) with the diffusion coefficients $D_{\mathrm{N@C_{60}\ in\ CS_2}} = 1.22 \times 10^9 \mathrm{m^2 s^{-1}}$, and $D_{\mathrm{N@C_{60}\ in\ 1-chloro}} = 1.41 \times 10^9 \mathrm{m^2 s^{-1}}$. These values for D are based on the Stokes–Einstein (SE) relation for the diffusion of spheres in fluids:'

$$D = \frac{k_B T}{6\pi\eta r} \tag{2}$$

where k_B is Boltzmann constant, T is the temperature, η is the viscosity and r is the molecular radius. Parameters used for the calculations of D are a C_{60} molecular radius of 0.51 nm [31], and a viscosity of 1-chloronaphthalene and CS_2 of 3.02 mPa s [32] and 0.35 mPa s [33], respectively. It is evident from the results of Fig. 6a that the SE relation provides a very good description of this molecule's motion. Other previous experiment of relevance using neutron scattering found $D_{C_{60}\ in\ CS_2} = 1.04 \times 10^{-9}\ \mathrm{m^2\ s^{-1}}$ (at 293 K) [34], which is a bit smaller than the value predicted by the SE relation ($1.22 \times 10^{-9}\ \mathrm{m^2\ s^{-1}}$). Measurements of C_{60} in benzene employing PGSE NMR found $D_{C_{60}\ in\ benzene} = 0.83 \times 10^{-9}\ \mathrm{m^2\ s^{-1}}$ [31], which is a bit larger than the SE prediction for that solvent ($0.67 \times 10^{-9}\ \mathrm{m^2\ s^{-1}}$) [31]. In the case of the trityl water solution, the theoretical graph represents a linear regression fitting that resulted in the measured $D_{\mathrm{trityl\ in\ H_2O}} = 6.51 \times 10^{-10} \mathrm{m^2\ s^{-1}}$. No prior data was found for the diffusion constant of trityl in water, but it is reasonable based on molecular size and solvent properties.

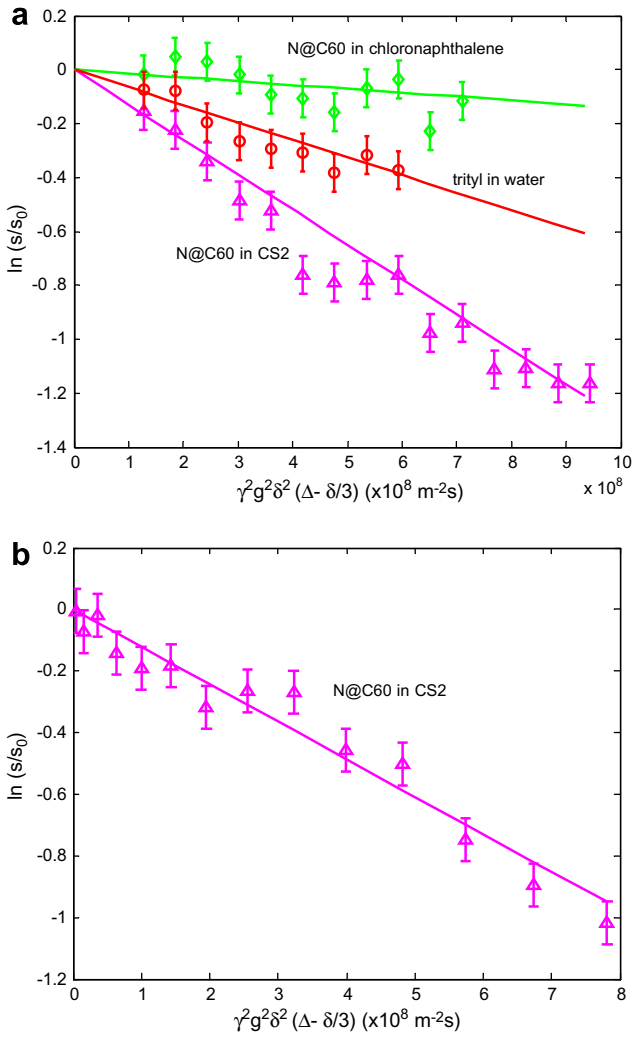

Fig. 6. (a) Stejskal-Tanner plot of the stimulated echo's ln magnitude as a function of the factor $q = \gamma^2 g^2 \delta^2 (\Delta - \delta/3)$ for N@C_{60} in 1-chloronaphthalene (◇) and CS_2 (Δ) and for trityl in water (o). The values of q were varied by changing τ_1 in the pulse sequence and were calculated on the basis of the true integral of the half-sine gradient pulse. (b) Similar plot as (a) but for N@C_{60} in CS_2 where in this experiment the values of q were varied by changing the amplitude of the peak g value while keeping all other parameters of the pulse sequence constant.

The second type of measurement employed fixed values of τ_1 and τ_2 with varying gradient magnitude. In this type of experiment, the sample is subjected to increasing pulsed-gradient values, leading to increased signal decay due to the effects of diffusion and the unwanted effects of the residual transient fields. In order to eliminate the unwanted contributions to the echo decay, we considered the results of the 1-chloronaphthalene sample (where the predicted diffusion decay is small) as a reference and used them to normalize the measurements of the N@C_{60} in CS_2 sample. The results of this type of measurement, for τ_2 = 2.5 μs, τ_1 = 40 μs and gradient values of up to 50 T/m, are shown in Fig. 6b. The theoretical graph was plotted using Eq. (1) with the same diffusion coefficient as in Fig. 6a.

3.3. Discussion

The results presented here clearly demonstrate that PGSE can be applied in conjunction with the ESR technique to the direct

measurement of motion of spin systems and stable radicals in liquids. If we consider the trityl in water as an example (where we obtained $6.51 \times 10^{-10} m^2 s^{-1}$), the current system capabilities can typically enable the measurement of motions of $\sim \sqrt{4Dt} = 0.32$ μm during a period of ~40 μs. Shorter times, down to ~10 μs, can be employed to measure smaller motions, but with lower accuracy (because the echo attenuation due to the diffusion-related term in Eq. (1) would become small with respect to T_1- and/or T_2-related attenuation), while larger times of up to 200 μs can be used to measure slower processes. For example, for the sample of $N@C_{60}$ in 1-chloronaphthalene, the diffusion length after 10 μs is only ~75 nm, which is about the limit of our experimental setup. Based on that reasoning, the rough borderline of present system capabilities, employing freely diffusing paramagnetic species such as trityl and $N@C_{60}$ in common solvents, is shown in solid green line in Fig. 1. The noise in the measurements of these samples, which contained $\sim 10^{13}$ spins (see 2.1), was not a limiting factor for our resonator, which can reach a sensitivity of $\sim 10^7$ spins [35]. However, the long-term signal stability (which causes signal variations between point to point on the graphs of Fig. 6) and the residual transient fields were a problem in the present setup. The current range of PGSE ESR capabilities can thus be greatly extended with future improvements such as the use of a much smaller probe for operation at 35 or 60 GHz (enabling larger gradient strength and employing smaller samples), means for a more effective cancellation of transient magnetic field effects, and the combination of PGSE ESR with ESR micro-imaging [28]. These upgrades would enable to fully realize the potential of PGSE ESR, as roughly plotted in Fig. 1 with dashed green line. For example, motions of ~6 nm is a time scale of ~100 ns (which would require gradients of ~500–1000 T/m) can be considered as a practical near future lower limit for the present probe configuration, while on the other hand, motions of ~6 μm with in a time scale of ~1 ms can be considered as an upper limit (based on the maximum T_1 of available samples).

PGSE complements the capabilities of PGSE NMR and can thus be applied to a variety of applications in biophysics and material science. In principle, this can be done with 'stand alone' stable radicals such as those employed above or with spin-labelled molecules. The capability to probe much shorter times than NMR can be valuable, for example, for the measurement and characterization of porous media (commonly found in biology) with sub-micron pores in an aqueous environment. (With NMR, in the milliseconds time scale, it is very difficult to characterize restricted motions in that length scale.) Here, the theoretical foundations laid down by the NMR community (e.g. [4]) can be of immediate use in characterizing complex cases such as anisotropic diffusion and diffusion in multichannel porous structures. Furthermore, the uniqueness of the ESR signal that can be attributed to a specific molecule can be used to differentiate between different types of motions of several species inside different compartments of complex or biological samples (while the NMR signal is in most cases attributed to the indistinguishable water signal). When the capabilities of PGSE are more fully realized, one may address issues such as large-scale 3D intramolecular dynamics of proteins or larger supra-molecular structures (e.g. [16]), or characterizing different types of protein motions in non-homogenous cellular membrane [11].

In conclusion, the gate that was opened up in this work could be greatly expanded by subsequent developments, which should enable monitoring unique processes of interest that are currently beyond the reach of the present capabilities of optical and NMR-based methodologies.

Acknowledgments

This work was partially supported by Grants # 169/05 and # 1143/05 from the Israeli science foundation, by Grant 2005258 from the BSF foundation, by grant form the European research Council (ERC), and by the Russell Berrie Nanotechnology Institute at the Technion. A.B. acknowledges Prof. Jack Freed for providing inspiration for this work.

References

[1] P.T. Callaghan, Principles of Nuclear Magnetic Resonance Microscopy, Oxford University Press, Oxford, 1991.
[2] J.E. Tanner, J. Chem. Phys. 52 (1970) 2523.
[3] G.A. Barrall, L. Frydman, G.C. Chingas, Science 255 (1992) 714.
[4] P.T. Callaghan, A. Coy, D. Macgowan, K.J. Packer, F.O. Zelaya, Nature 351 (1991) 467.
[5] V. Kukla et al., Science 272 (1996) 702.
[6] C. Parravan, J. Baldesch, M. Boudart, Science 155 (1967) 1535.
[7] H. Wassenius, P.T. Callaghan, J. Mag. Res. 169 (2004) 250.
[8] C. Pappas, F. Mezei, A. Triolo, R. Zorn, Phys. B – Cond. Matt. 356 (2005) 206.
[9] N.B. Cole, C.L. Smith, N. Sciaky, M. Terasaki, M. Edidin, J. LippincottSchwartz, Science 273 (1996) 797.
[10] P. Schwille, U. Haupts, S. Maiti, W.W. Webb, Biophys. J. 77 (1999) 2251.
[11] T. Schmidt, G.J. Schutz, W. Baumgartner, H.J. Gruber, H. Schindler, Proc. Nat. Acad. Sci. USA 93 (1996) 2926.
[12] M. Tehei et al., Proc. Nat. Acad. Sci. USA 104 (2007) 766.
[13] J. Enderlein, I. Gregor, D. Patra, T. Dertinger, U.B. Kaupp, Chemphyschem 6 (2005) 2324.
[14] Z. Petrasek, P. Schwille, Biophys. J. 94 (2008) 1437.
[15] O.F. Lange et al., Science 320 (2008) 1471.
[16] G.C.K. Roberts, Biochem. Soc. Trans. 34 (2006) 971.
[17] P.P. Borbat, A.J. Costa-Filho, K.A. Earle, J.K. Moscicki, J.H. Freed, Science 291 (2001) 266.
[18] F. Caruso, F. Grieser, A. Murphy, P. Thistlethwaite, R. Urquhart, M. Almgren, E. Wistus, J. Am. Chem. Soc. 113 (1991) 4838.
[19] D.D. Thomas, W.F. Carlsen, L. Stryer, Proc. Nat. Acad. Sci. USA 75 (1978) 5746.
[20] L. Yong et al., J. Mag. Res. 152 (2001) 156.
[21] A.C. Wright, H. Bataille, H.H. Ong, S.L. Wehrli, H.K. Song, F.W. Wehrli, J. Mag. Res. 186 (2007) 17.
[22] G.G. Maresch et al., J. Chem. Phys. 91 (1989) 4543.
[23] A. Feintuch, T. Tashma, A. Grayevsky, J. Gmeiner, E. Dormann, N. Kaplan, J. Mag. Res. 157 (2002) 69.
[24] J.H. Freed, Ann. Rev. Biophy. & Biomol. Str. 23 (1994) 1.
[25] T. Almeida Murphy, T. Pawlik, A. Weidinger, M. Hohne, R. Alcala, J.M. Spaeth, Phys. Rev. Lett. 77 (1996) 1075.
[26] W. Harneit, K. Huebener, B. Naydenov, S. Schaefer, M. Scheloske, Phys. Status Solidi B 244 (2007) 3879.
[27] P. Jakes, K.P. Dinse, C. Meyer, W. Harneit, A. Weidinger, Phys. Chem. Chem. Phys. 5 (2003) 4080.
[28] A. Blank, C.R. Dunnam, P.P. Borbat, J.H. Freed, Appl. Phys. Lett. 85 (2004) 5430.
[29] M.S. Conradi, A.N. Garroway, D.G. Cory, J.B. Miller, J. Mag. Res. 94 (1991) 370.
[30] A. Blank, C.R. Dunnam, P.P. Borbat, J.H. Freed, J. Mag. Res. 165 (2003) 116.
[31] T. Kato, K. Kikuchi, Y. Achiba, J. Phys. Chem. 97 (1993) 10251.
[32] T.M. Aminabhavi, V.B. Patil, J. Chem. & Eng. Data 43 (1998) 504.
[33] T. Nakagawa, J. Mol. Liq. 63 (1995) 303.
[34] H.E. Smorenburg, R.M. Crevecoeur, I.M. Deschepper, L.A. Degraaf, Phys. Rev. E 52 (1995) 2742.
[35] A. Blank, J.H. Freed, N.P. Kumar, C.H. Wang, J. Contr. Release 111 (2006) 174.
[36] A. Schweiger, G. Jeschke, Principles of Pulse Electron Paramagnetic Resonance, Oxford University Press, Oxford, UK, 2001.